EBioMedicine 26 (2017) 47–59

Contents lists available at ScienceDirect

EBioMedicine

journal homepage: www.ebiomedicine.com

Research Paper

An Elastomeric Polymer Matrix, PEUU-Tac, Delivers Bioactive Tacrolimus Transdurally to the CNS in Rat

Yolandi van der Merwe [a,c,d], Anne E. Faust [a,c], Ian Conner [a,c], Xinzhu Gu [c,e], Firuz Feturi [c,f], Wenchen Zhao [f], Bianca Leonard [c,g], Souvik Roy [c,g], Vijay S. Gorantla [c,j], Raman Venkataramanan [c,f,k], Kia M. Washington [c,h,i], William R. Wagner [c,d,e], Michael B. Steketee [a,b,c,g,*]

[a] Department of Ophthalmology, University of Pittsburgh, Pittsburgh, PA, United States
[b] Center for Neuroscience, University of Pittsburgh, Pittsburgh, PA, United States
[c] McGowan Institute for Regenerative Medicine, University of Pittsburgh, Pittsburgh, PA, United States
[d] Department of Bioengineering, University of Pittsburgh, Pittsburgh, PA, United States
[e] Department of Surgery, University of Pittsburgh, Pittsburgh, PA, United States
[f] Department of Pharmaceutical Sciences, University of Pittsburgh, Pittsburgh, PA, United States
[g] Department of Neuroscience, University of Pittsburgh, Pittsburgh, PA, United States
[h] Department of Plastic Surgery, University of Pittsburgh, Pittsburgh, PA, United States
[i] VA Pittsburgh Healthcare System, Pittsburgh, PA, United States
[j] Departments of Surgery, Ophthalmology and Bioengineering, Wake Forest School of Medicine, Wake Forest Institute of Regenerative Medicine, Winston Salem, NC, United States
[k] Department of Pathology, University of Pittsburgh, Pittsburgh, PA, United States

ARTICLE INFO

Article history:
Received 1 September 2017
Received in revised form 10 November 2017
Accepted 20 November 2017
Available online 24 November 2017

Keywords:
Tacrolimus
FK506
Retinal ganglion cell
CNS
Axon regeneration
Optic nerve

ABSTRACT

Central nervous system (CNS) neurons fail to regrow injured axons, often resulting in permanently lost neurologic function. Tacrolimus is an FDA-approved immunosuppressive drug with known neuroprotective and neuroregenerative properties in the CNS. However, tacrolimus is typically administered systemically and blood levels required to effectively treat CNS injuries can lead to lethal, off-target organ toxicity. Thus, delivering tacrolimus locally to CNS tissues may provide therapeutic control over tacrolimus levels in CNS tissues while minimizing off-target toxicity. Herein we show an electrospun poly(ester urethane) urea and tacrolimus elastomeric matrix (PEUU-Tac) can deliver tacrolimus trans-durally to CNS tissues. In an acute CNS ischemia model in rat, the optic nerve (ON) was clamped for 10s and then PEUU-Tac was used as an ON wrap and sutured around the injury site. Tacrolimus was detected in PEUU-Tac wrapped ONs at 24 h and 14 days, without significant increases in tacrolimus blood levels. Similar to systemically administered tacrolimus, PEUU-Tac locally decreased *glial fibrillary acidic protein* (*GFAP*) at the injury site and increased *growth associated protein-43* (*GAP-43*) expression in ischemic ONs from the globe to the chiasm, consistent with decreased astrogliosis and increased retinal ganglion cell (RGC) axon growth signaling pathways. These initial results suggest PEUU-Tac is a biocompatible elastic matrix that delivers bioactive tacrolimus trans-durally to CNS tissues without significantly increasing tacrolimus blood levels and off-target toxicity.

1. Introduction

In adult mammals, central nervous system (CNS) injury remains a persistent experimental and clinical challenge. Trauma to CNS tissues triggers a pro-inflammatory innate immune response that leads to secondary tissue damage, injury site expansion, and cellular and extracellular matrix (ECM) remodeling (Horn et al., 2008). This default healing response contributes to failed axon regeneration (Peruzzotti-Jametti et al., 2014; Tang et al., 2001) and promotes scar tissue formation (Silver and Miller, 2004), often leading to irreversible CNS neuron death (Russo et al., 2016) and permanently lost neurological function. Thus, combinatorial approaches are needed that can positively modulate the innate immune response to promote functional tissue remodeling over scarring while also providing key neuroprotective and neuroregenerative support to CNS neurons.

Tacrolimus, also called FK506, is a macrolide immunosuppressive drug initially derived from *Streptomyces tsukubaensis* (Prograf ® Astellas, NJ) (Petan et al., 2008) widely used clinically to prevent organ transplant rejection (Starzl et al., 1989) as well as to treat various dermatologic (Madan and Griffiths, 2007) and autoimmune diseases (Chen et al., 2017). Tacrolimus binds to FK506-binding protein (FKBP)

* Corresponding author at: Department of Ophthalmology, Center for Neuroscience, McGowan Institute for Regenerative Medicine, University of Pittsburgh, 450 Technology Drive Suite 300, Pittsburgh, PA 15213, United States.
E-mail addresses: SteketeeM@UPMC.edu, Stek0323@gmail.com (M.B. Steketee).

https://doi.org/10.1016/j.ebiom.2017.11.017

receptors of the immunophilin family, which comprises at least 15 members in humans. In humans, tacrolimus is thought to prevent organ transplant rejection by suppressing T-cell activation *via* binding to FKBP12 (Xu et al., 2002). In the CNS, FKBPs are widely expressed by numerous cell types, including both neurons and glia, with different cellular populations exhibiting distinct FKBP subtype expression patterns and pharmacokinetics. In the CNS, tacrolimus is hypothesized to modulate the innate immune response by reducing neutrophil and macrophage infiltration and microglial (Zawadzka et al., 2012) and astrocyte activation (Zawadzka and Kaminska, 2005; Szydlowska et al., 2006; Liu et al., 2011), subsequently reducing oxidative stress, secondary damage, and injury site expansion (Fukuta et al., 2015).

Experimentally, tacrolimus can also provide both neuroprotective and neuroregenerative benefits to CNS neurons. Although FKBPs are widely expressed by CNS neurons, tacrolimus appears to modulate neuronal activities by multiple mechanisms, including both FKBP-dependent and FKBP-independent routes (Gold et al., 2005). After optic nerve (ON) ischemia in rats, tacrolimus increases retinal ganglion cell (RGC) survival by suppressing apoptotic signaling (Freeman and Grosskreutz, 2000). After spinal cord injury in rats, tacrolimus increases axon growth and the expression of *growth associated protein-43 (GAP43)*, an axon growth marker (Wang and Gold, 1999; Madsen et al., 1998) and has been reported to improve functional recovery (Voda et al., 2005). In recent studies, tacrolimus has been shown to reduce ischemia reperfusion injury in white matter after cerebral artery occlusion surgery (Fukuta et al., 2015) and to decrease apoptosis in hippocampal neurons (Sharifi et al., 2012). However, most experimental studies have relied on systemic administration to deliver tacrolimus to CNS tissues (Sharifi et al., 2012; Fukuta et al., 2015). Tacrolimus is highly lipophilic and thus accumulates in fatty tissues throughout the body, including the myelin-based white matter in the CNS. However, systemic delivery to CNS tissues is complicated by preferential uptake by other organs, which requires higher systemic doses to effectively increase tacrolimus in CNS tissues. These increases in systemic tacrolimus often lead to often life-threatening toxicity in other tissues and organs.

Clinically, tacrolimus is typically administered systemically either orally or by injection (Varghese et al., 2014; Yamazoe et al., 2014). The chemical properties of tacrolimus require careful consideration with regard to systemic administration. The method of administration, frequency, and dosage, must be carefully monitored to maintain effective therapeutic tissue levels without inducing toxicity in off-target tissues. Improperly regulated systemic levels can lead to a number of life-threatening side effects, including, but not limited to, diabetogenicity, nephrotoxicity, neurotoxicity, and oncogenicity (Randhawa et al., 1997; Starzl et al., 1989). Moreover, tacrolimus administration is further complicated by the number and distribution of FKBP binding proteins. Tacrolimus acts on at least 15 FKBP binding receptors in humans differentially expressed by cellular populations in different tissues and organs. Therefore, tacrolimus administration must be carefully optimized to maintain effective concentrations within the tissues of interest to maximize efficacy while minimizing toxic side-effects both to targeted and to non-targeted cellular populations and tissues. Thus, strategies are being developed to deliver tacrolimus locally. Local delivery approaches include hydrogels (Gabriel et al., 2016), inhalants (Deuse et al., 2010), and micelle (Lapteva et al., 2014) or polymer encapsulation technologies (Tajdaran et al., 2015). However, these technologies are limited for many CNS applications due to ineffective and/or inconsistent tacrolimus delivery to specific CNS tissues, incompatible mechanical properties, and the inability to remain intact and/or localized to the injury site.

To deliver tacrolimus locally and controllably to CNS tissues, this study developed a biodegradable and elastic matrix using poly(ester urethane) urea (PEUU) (Guan et al., 2002). PEUU polymers have desirable mechanical characteristics, including high elasticity and strength, good cell-adhesive properties, and controllable biodegradation, all of which can be tuned to match the tissue of interest. By modifying a previously developed PEUU electrospinning platform (Stankus et al., 2004), tacrolimus and PEUU were successfully blended into PEUU polymer matrices. This method allowed precise control over both the PEUU and tacrolimus concentrations as well as control over the size and the thickness of the PEUU-Tac matrices. PEUU-Tac material properties and release kinetics were analyzed *in vitro*. The dose-dependent effects of tacrolimus on primary RGC viability, toxicity, and differentiation were analyzed *in vitro*. Finally, PEUU-Tac matrices were used as ON wraps to analyze local, trans-dural tacrolimus delivery both to CNS tissues and to the blood in an acute ON ischemia model in rat.

2. Materials and Methods

2.1. Animals

Sprague-Dawley rats were purchased from Charles River Laboratories (Wilmington, MA). Animals were housed and maintained according to the guidelines set forth by the University of Pittsburgh Institutional Animal Care and Use Committee (IACUC) and the DOD Animal Care and Use Review Office (ACURO). All procedures complied with the American Association for the Accreditation of Laboratory Animal Care (AALAC).

2.2. Retinal Ganglion Cells

Primary RGCs were isolated from female and male postnatal day three (P3) Sprague-Dawley rat pups, purified by immunopanning, and cultured in NB-SATO media as described (Barres et al., 1988). RGCs were seeded ($5 \times 10^3/cm^2$) in cell culture plates coated with poly-D-lysine (70 kDa, 10 μg/ml; Sigma-Aldrich Corp., St. Louis, MO, USA) and laminin (2 μg/ml, Sigma-Aldrich Corp.). Tacrolimus (Invitrogen) was diluted in 100% EtOH to make a 20 mM stock. The tacrolimus stock was then diluted in NB-SATO as specified and the RGC cultures maintained at 37 °C in 10% CO_2 for 3 days *in vitro* (DIV).

2.3. RGC Viability

Viability was analyzed after 3 DIV using a calcein and propidium iodide based live/dead kit per manufacturer's instructions (Life Technologies, R37601). For analysis, the first five non-overlapping fields of view per well, moving from the left well edge, were imaged at 20× using standard epi-fluorescence fluorescein and rhodamine filter sets (Zeiss, Axio Observer). Experimentally blinded individuals analyzed live and dead cells using ImageJ (National Institutes of Health, Bethesda, MD, USA). Data represent triplicates from four experimental repeats, totaling at least 27 fields of view and at least 300 neurons per group as previously described (Faust et al., 2017). Significance between groups was determined by one-way analysis of variance (ANOVA) as noted in Section 2.13.

2.4. RGC Neurite Growth

After 3 DIV, RGCs were fixed with 4% paraformaldehyde (Alfa Aesar; 30525-89-4) in PBS, washed with PBS (2×), and permeabilized with 0.2% triton X-100 in PBS for 15 min. After blocking for 1 h (1% BSA in PBS, Fisher Scientific), the RGCs were incubated with anti-β III tubulin (1:300, TUJ-1, Millipore, RRID: AB 570918) at 4 °C overnight, washed in PBS (3×), incubated with a FITC-rabbit anti-chicken IgY H + L secondary (1:150, #31501, Thermo Scientific) for 3 h, washed with PBS (3×), counterstained with the nuclear marker DAPI (1:3000, Invitrogen, D1306) for 20 min at room temperature, and washed in PBS (2×, 5 min each). The RGCs were imaged randomly as described above and neurite growth measured by blinded individuals as described (Steketee et al., 2011) using the ImageJ plugin, NeuronJ (National Institutes of Health, Bethesda, MD, USA). The first ten non-contacting RGCs encountered, moving right from the left edge of the well, were analyzed from

triplicate wells in each of three independent experimental repeats, totaling at least 90 neurons per condition. Significance between groups was determined by ANOVA as noted in Section 2.13.

2.5. PEUU-Tac

Poly(ester urethane) urea (PEUU) was synthesized from polycaprolactone diol (Mn = 2000), 1,4-diisocyanatobutane and putrescine, as described (Guan et al., 2002) and PEUU-Tac matrices were fabricated by single stream electrospinning as described (Hong et al., 2011). Briefly, 10 mg or 20 mg of tacrolimus was dissolved in 500 μL of 1,1,1,3,3,3-hexafluoroisopropanol (HFIP). Each tacrolimus solution was mixed with 0.45 g PEUU (12% w/v in HFIP) and electrospun onto a rotating stainless-steel mandrel (19 mm diameter) by feeding through a charged capillary at a rate of 3 ml/h. The mandrel was located 17 cm from the tip of the capillary and the voltage between the capillary and the mandrel was 19 kV. PEUU-Tac matrices were sterilized under UV light overnight and then with ethylene oxide (ETO) before use.

2.6. PEUU-Tac Release Kinetics

To determine tacrolimus release rate, PEUU-Tac matrices were cut into three equal weight sections (15 mg) and each section was placed in 25 ml of 0.5% Cremephor EL (C5135, Sigma, St. Louis, MO) in PBS (CrEL-PBS) (Howrie et al., 1985) in Sigmacote (SL2, Sigma, St. Louis, MO) treated 50 ml glass beakers with gentle agitation (60 RPM, Thermo Labline 2314 Orbital Shaker). At the indicated time points ranging from 1 h to 14 days, 300 μl was removed for analysis and then replaced with 300 μl of fresh CrEL-PBS. For each sample, 50 μl was mixed with 450 μl of blood and analyzed by Ultra performance liquid chromatography (UPLC)-tandem mass spectrometry as described in section 2.11. Three additional 50 ml glass beakers were coated with Sigmacote. One PEUU-Tac section was placed in each beaker with 25 ml CrEL-PBS with gentle agitation (60 RPM, Thermo Labline 2314 Orbital Shaker) for 24 h. The three PEUU-Tac sections were removed from the CrEL-PBS solution and each placed in 5 ml of HFIP with gentle agitation for 5 min to dissolve the PEUU scaffold. Three fresh PEUU-Tac sections of equal weight to the pre-release scaffold weight were also placed in 5 ml HFIP. The tacrolimus concentration was then measured for each sample by UPLC-tandem mass spectrometry as in section 2.11. Significance between groups was determined by ANOVA as noted in Section 2.13.

2.7. PEUU and PEUU-Tac Degradation

The degradation rate of PEUU-Tac was analyzed at 37 °C in PBS as described (Hong et al., 2010). Briefly, equal size samples (10 × 5 × 0.1 mm) were cut from an unloaded PEUU matrix, 10 mg or 20 mg tacrolimus loaded PEUU-Tac and placed in 15 ml of PBS in a 20 ml vial. At each time point, the samples were removed from the buffer, washed with deionized water, and dried under vacuum at room temperature for 3 to 4 days before weighing to determine the mass, using the equation:

$$\text{Mass Remaining}\ (\%) = \left(\frac{m_d}{m_{orig}}\right) \cdot 100$$

where m_d is the sample after drying and m_{orig} is the original mass. After weighing, each sample was placed in fresh PBS. The time in PBS indicates the total time in PBS, independent of the drying time. For visualization, the PEUU matrices were sputter-coated with gold/palladium and imaged using standard scanning electron microscopy methods (SEM; JSM-6330F, JEOL USA). Data represent triplicates from three experimental repeats. The average mass is reported with the error bars indicating one standard deviation. Significance between groups was determined by ANOVA as noted in Section 2.13.

2.8. PEUU-Tac Mechanical Properties

To test the mechanical properties of PEUU or PEUU-Tac, each matrix was cut into a dumbbell shape geometry (ASTM D1708) using a custom-made dog-bone cutting die with a 2.5 mm width, a 10 mm gauge length, and a total length of 20 mm. PEUU and PEUU-Tac tensile properties were analyzed by uniaxial tensile testing using an MTS Insight (MTS Systems Corporation, MN, USA) with a 10 N (0.01 N resolution) load cell at room temperature. The samples were extensionally deformed at 10 mm/min, according to ASTM D638M. Young modulus was calculated by finding the initial slope of the stress *versus* strain curve ($0 < \varepsilon < 10\%$) using linear regression. The ultimate stress was determined as the maximum stress and the strain-at-break recorded as the strain at the point where the force became zero. The averages and error bars, indicating one standard deviation, are reported. Data represent triplicates from three experimental repeats. Significance between groups was determined by ANOVA as noted in Section 2.13.

2.9. ON Ischemia and PEUU-Tac

Animals were anesthetized by injecting a 45:10 mg/kg ketamine/xylazine cocktail intraperitoneally. The ON was exposed by making a small incision in the conjunctiva and then blunt dissecting a nearly bloodless plane back to the ON using #5 jeweler forceps. The muscle and connective tissues around the ON were gently separated to expose the ON sheath. Using a Yasargil aneurysm clip (Aesculap FT252T), the right ON was clamped approx. 2 mm behind the globe for 10 s (Sarikcioglu et al., 2007). After clamping, the ophthalmic artery was visualized to confirm integrity. A subset of animals (n = 5) had the ON sheath fenestrated at the clamp site by making a 1–2 mm incision using an ultra-sharp scalpel (#681.01, Oasis Medical). For animals receiving PEUU-Tac, a 2 × 5 mm section of 10 mg PEUU-Tac was wrapped around the injury site and sutured to itself and to the sheath. The conjunctiva was then sutured closed and antibiotic ointment (NDC 24208-780-55, Gentamicin, Bausch & Lomb, Tampa, Florida) applied to the eye. In total, forty-six animals were used. The experimental groups included: 1. Injured. Nine animals received only ischemia to the right ON. 2. Injured, PEUU-Tac. After ischemia to the right ON of 14 animals, a 2 mm × 5 mm section of 10 mg PEUU-Tac was sutured around the injury site (no fenestration). 3. Injured, PEUU-Tac (fenestrated). After ischemia to the right ON of five animals, the ON sheath was fenestrated as described above before a 2 mm × 5 mm section of 10 mg PEUU-Tac was sutured around the injury site. 4. Systemic. After ischemia to the right ON, nine animals were injected intraperitoneally with tacrolimus (2.2 mg/kg/day) for 14 days with the first injection administered immediately after surgery. 5. Nine animals served as sham surgery controls. Five animals per group were used for tacrolimus tissue levels analysis and four were used for immunohistochemistry. The injured, PEUU-Tac group had five additional animals that were used for Tac tissue level analysis at 24 h. Power analysis was used to determine sample size. The number of experimental animals was determined using G*power software (G*power software 3.1.9.2, Germany). We calculated the effect size to be 0.6 according to our previous experiments. Power analysis for ANOVA dictates n = 4 animals for histological analysis and n = 5 animals for tacrolimus tissue levels per group for *in vivo* studies to achieve 80% power for $\alpha = 0.05$. Animals were randomly assigned to groups by an experimentally blinded animal technician.

2.10. Tacrolimus Blood Tissue Analysis

Twenty-four hours after surgery, 500 μl of blood was drawn *via* the tail vein. Additionally, at 24 h, four PEUU-Tac treated animals were sacrificed and the ONs and retinas collected. At 14 days, the remaining thirty-six animals were sacrificed and blood, retinas, and ONs collected. Tacrolimus tissue levels were analyzed from five animals per group and the remaining four animals per group were used for

immunohistochemistry. The blood was collected in BD Microtainer blood collection tubes (Becton Dickinson, 363,706) pre-coated with EDTA to avoid coagulation, and stored at 4 °C until analysis. Retinas and ONs were weighed, homogenized in 100% methanol (MeOH) using a Mini-BeadBeater-1 sonicator (Mini-BeadBeater-16, Thomas Scientific), and left overnight to ensure complete tacrolimus extraction. The homogenate was centrifuged at 2100 ± 100 RPM for 10 min, the MeOH transferred to a microcentrifuge tube, and evaporated completely using a vacufuge (Eppendorf Vacufuge Plus 5305 Concentrator Vacuum). The residue was then reconstituted in 1 ml of naïve rat blood prior to quantification as described below.

2.11. Tacrolimus Quantification by UPLC-tandem Mass Spectrometry

Tacrolimus was analyzed by UPLC (Nova-pack® C18 column, 2.1 × 10 mm cartridge (Waters #186003523)) as described (Solari et al., 2009; Unadkat et al., 2017). Briefly, standard curves and quality control blood samples were prepared using dry tacrolimus (tlrl-fk5, Invivogen). For each sample, 50 μL blood was added to a conical centrifugation tube, followed by 200 μL zinc sulfate heptahydrate (ZnSO4·7H2O) to precipitate the blood proteins, and 500 μL ascomycin (20 ng/l in acetonitrile) as an internal standard. The samples were vortexed for 2 min at 3000 RPM, centrifuged for 3 min at 13000 RPM, and the supernatants collected in LCMS vials (60180-508, Thermo Scientific). Analysis was done using a fully validated, reverse phase UPLC method for detecting tacrolimus in blood with an injection volume of 10 μL. Analytes were separated using a gradient elution consisting of an aqueous mobile phase (95% H2O/5% MeOH) and an organic mobile phase (100% MeOH), at a flow rate of 0.6 ml per min. To optimize ionization and enhance the chromatographic output quality, both mobile phases contained 0.1% formic acid (CH_2O_2) and 2 mM ammonium acetate. Both intra- and inter-day precision were shown to be acceptable (C.V. <10%, n = 3) at concentrations of 4.3, 15.7, and 24.6 ng/ml. Results are expressed as tacrolimus in ng/g of tissue or ng/ml of blood. For animal blood and tissue tacrolimus levels, data represent triplicates from at least five animals per condition analyzed by ANOVA as noted in Section 2.13.

2.12. Immunohistochemistry

For immunohistochemistry, tissues were fixed in 4% paraformaldehyde for 4 h, cryoprotected in 30% sucrose for 4 h, embedded in optical cutting temperature (OCT) medium (Tissue-Tek; Miles Inc., Elkhart, IN) and stored at 4 °C overnight before freezing in liquid nitrogen. Embedded tissues were stored at −80 °C prior to cryostat sectioning (15 μm thickness). ON sections were permeabilized with 0.2% triton X-100 in PBS for 15 mins, washed in PBS (2×), blocked for 1 h (1% BSA in PBS, BP9706100, Fisher Scientific), and washed in PBS (2×). ON sections were labeled with anti-glial fibrillary acidic protein antibody (Anti-GFAP, 1:500, Abcam, AB7260, RRID:AB_296804) or anti-growth associated protein 43 (Anti-GAP-43GAP-43, 1:500, Abcam, AB16053, RRID:AB_598153), and DAPI (1:2000, Thermo Scientific, 62,247). The sections were imaged and pixel intensities measured by experimentally blinded individuals using ImageJ as described (Mccloy et al., 2014). Briefly, fifteen ROIs of 100 × 100 pixels were drawn around the crush site (*GFAP*) and distal to the crush site (*GAP-43*). Four ROIs were drawn on the image background. The area, mean fluorescence, and integrated density for each image were analyzed using the following formula: CTCF = integrated density − (area × mean background fluorescence). Data represent triplicates from three experimental repeats analyzed by ANOVA as noted in Section 2.13.

2.13. Statistical Analysis

All analyses were done by experimentally blinded individuals. To determine significance between groups ($p < 0.05$), ANOVA was used in conjunction with a Tukey's post-hoc test using SPSS Statistical Analysis Software (IBM, Chicago, IL, USA). All error bars represent standard error of the mean (SEM) unless noted otherwise.

3. Results

3.1. Tacrolimus Regulates RGC Viability Bi-modally

Previous studies indicate tacrolimus has both neuroprotective and neuroregenerative effects on CNS neurons, including RGCs *in vitro* (Rosenstiel et al., 2003) and *in vivo* (Freeman and Grosskreutz, 2000). However, the effective concentration ranges on RGC viability and growth have not been reported for primary RGCs *in vitro*. To determine the dose-dependent effects of tacrolimus on RGC toxicity *in vitro*, RGCs were cultured in tacrolimus concentrations, ranging from 0.1 to 100 μM (Fig. 1b). Below 0.1 μM, RGC viability was unchanged. At 0.1 μM, RGC viability was 66%, or 94% of the vehicle control, which is in the typical range for primary RGCs cultured *in vitro*. Over 0.1 μM, RGC viability initially increased to a maximum of 91% viable, 21% greater than control, at 0.5 μM, before decreasing dose-dependently to 0% at 75 μM. Lethal dose (LD) response analysis was conducted by plotting the data points on a semi-logarithmic graph and then using non-linear regression to generate a dose response curve, which indicated an LD_{50} = 24.2 μM (Fig. 1c).

3.2. Effect of Tacrolimus on RGC Axon Growth

To determine tacrolimus effects on RGC neurite growth, RGCs were initially cultured at high density and total neurite growth, which included both axons and dendrites, was analyzed (Fig. 2b). The average total neurite growth per neuronal cell body was greatest at 5 nM but neurite growth did not follow a typical dose-response relationship. From 10 nM to 5 μM, total neurite growth remained largely unchanged before decreasing coordinately with viability to 0 at 75 μM. Thus, although 5 nM stimulated growth to the greatest extent, tacrolimus appears to support RGC neurite growth over a broad concentration range up to 5 μM *in vitro*.

In high-density cultures, the specific effects of tacrolimus on neurite growth, *i.e.* dendrite *vs.* axon growth or branching, is masked by neurite to neurite contact and fasciculation (Steketee and Tosney, 1999). Therefore, we analyzed the effects of 5 μM tacrolimus on total neurite growth, axon growth, and branching in non-contacting neurons, cultured in low-density cultures (Fig. 2c–e). In contrast to high-density cultures, tacrolimus increased total neurite growth by 66% and axon growth by 45% (Fig. 2b), whereas branching frequency was unchanged (Fig. 2c). Thus, the majority, 69%, of the total increase in neurite growth by tacrolimus is due to increased axon growth *in vitro*. These data provide a basis for identifying the receptors and the signaling pathways by which tacrolimus acts to differentially modulate neurite growth in CNS neurons, like RGCs.

3.3. Electrospun PEUU and PEUU-Tac Constructs

To construct a tacrolimus releasing matrix, a previously reported electrospinning protocol for PEUU (Stankus et al., 2004) was extended by electrospinning either 10 or 20 mg of tacrolimus blended with PEUU. Macroscopically, PEUU and 10 or 20 mg loaded PEUU-Tac matrices were off-white, pliable sheets, and indistinguishable from one another (Fig. 3a, inset). Microscopically, PEUU polymer fiber size and gross organization were also similar after elecrospinning. In both PEUU and PEUU-Tac matrices, scanning electron microscopy (SEM) revealed randomly organized polymer fibers with varied diameters (Fig. 3a). The average polymer fiber diameter was similar in all three matrices; unloaded PEUU fibers were 510 ± 130 nm and 10 or 20 mg loaded PEUU-Tac fibers averaged 560 ± 210 nm and 560 ± 160 nm, respectively. Thus, tacrolimus loading does not alter the gross

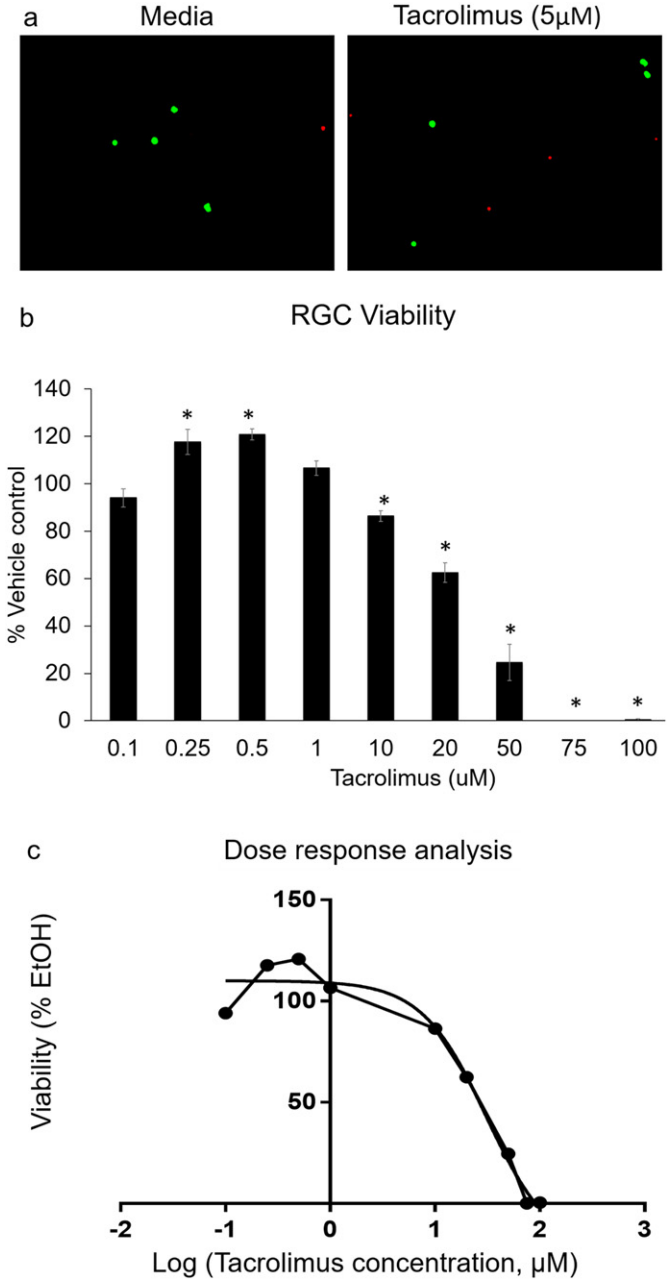

Fig. 1. Tacrolimus regulates RGC viability bi-modally in a concentration dependent manner. a. Representative images of live/dead stained RGCs grown in media or tacrolimus for 3 DIV. b. Initially, tacrolimus increased RGC cell viability up to approx. 120% of control at 0.5 μM. At higher concentrations, viability decreased dose dependently, returning to vehicle control values at approximately 1 μM. The actual % viable cells at each concentration after 3 DIV were as follows: 0.1 μM (94%), 0.25 μM (117%), 0.5 μM (120%), 1 μM (106%), 10 μM (86%), 20 μM (62%), 50 μM (24%), 75 μM (0%). c. Dose response curve for tacrolimus toxicity. The individual points represent the actual values and the curve represents the non-linear regression curve that indicates an LD50 = 24.2 μM. n ≥ 150 random neurons cultured in triplicate for at least 3 experimental repeats. Error bars represent the SEM. $^{*}p < 0.05$.

macroscopic appearance of PEUU matrices nor the microscopic organization and diameter of electrospun PEUU polymer fibers.

3.4. PEUU-Tac Release Kinetics

Both the 10 and the 20 mg PEUU-Tac matrices released tacrolimus at similar rates, yielding final concentrations proportional to their loading concentration (Fig. 3c). The 10 mg PEUU-Tac matrix yielded a maximum concentration of 11.56 μg/ml (14.5 μM) within the first 24 h and a final concentration that was not significantly different from the 24-hour time point of 9.53 μg/ml (11.3 μM) at 14 days. The 20 mg matrix released tacrolimus similarly, yielding a concentration of 20.4 μg/ml (24.3 μM) within the first 24 h and a final concentration of 23.7 μg/ml (28.2 μM) at 14 days that was also not significantly different from the 24-hour time point. Analysis of residual tacrolimus in PEUU-Tac matrices after 14 days showed that 85.7 ± 2.4% was released within 24 h and the remainder was retained in the matrix over the 14 day time point analyzed. Thus, both 10 mg and 20 mg PEUU-Tac matrices release tacrolimus at similar rates *in vitro* with near maximum concentrations reached in approximately 24 h without significant increases detected over the next 13 days analyzed.

3.5. PEUU-Tac Matrix Degradation In Vitro

To determine if tacrolimus loading alters PEUU matrix degradation, we analyzed the percent change in mass of unloaded PEUU and 10 or 20 mg loaded PEUU-Tac matrices over eight weeks (Hong et al., 2010). Changes in mass were similar for all three matrices (Fig. 3d). At 1, 2, and 5 weeks, mass was largely unchanged. However, between weeks five and eight the mass decreased similarly and significantly in all three matrices. Unloaded PEUU matrix was reduced to 31 ± 1% and PEUU-Tac, 10 and 20 mg tacrolimus loaded matrices, were reduced to 21 ± 9%, and 22 ± 18%, respectively. However, these similar changes in mass, were accompanied by distinct microscopic changes in PEUU fiber morphology that correlated with tacrolimus loading. At eight weeks, SEM showed polymeric fibers were less defined but still distinguishable in PEUU. However, PEUU-Tac lacked identifiable polymer fibrils (Fig. 3b). Thus, although changes in mass were similar, tacrolimus loading leads to a more rapid loss in polymeric fiber architecture. Despite these changes in polymer organization and losses in mass, the PEUU and PEUU-Tac matrices remained sufficiently intact to be handled manually after 8 weeks.

3.6. Mechanical Properties of PEUU-Tac

The stress-strain relationship, Young's modulus, ultimate stress, and strain at break were calculated for the PEUU, 10 and 20 mg PEUU-Tac matrices (Fig. 4). The stress-strain relationship is shown for each PEUU device (Fig. 4a). Tacrolimus loading did not significantly change Young's modulus. Unloaded PEUU was 25 ± 9 MPa, 10 mg PEUU-Tac was 19 ± 12 MPa, and 20 mg PEUU-Tac was 15 ± 11 MPa (Fig. 4b). Similarly, no significant difference in strain at break was observed between the PEUU (262 ± 21%), 10 mg (217 ± 67%), and 20 mg (222 ± 34%) matrices (Fig. 4c). However, ultimate stress was reduced significantly in tacrolimus loaded PEUU matrices compared to the unloaded matrix. PEUU ultimate stress was measured at 13 ± 4 MPa, 10 mg PEUU-Tac at 6 ± 0.5 MPa, and 20 mg PEUU-Tac at 6 ± 3 MPa (Fig. 4d).

3.7. PEUU-Tac in an Acute ON Ischemia in Rat

To determine if PEUU-Tac can deliver tacrolimus locally to CNS tissues trans-durally without significantly increasing blood levels, 10 mg PEUU-Tac matrices were used as nerve wraps after acute ON ischemia in rat (Fig. 5a). The ON was clamped using a Yasargil aneurism clip for 10 s and then either left untreated or wrapped with PEUU or PEUU-Tac around the injury site and sutured to itself and to the dura mater to prevent movement (Fig. 5b). In a subset of animals, the sheath was fenestrated at the injury site to expose the ON before applying the PEUU-Tac matrix. In these *in vivo* studies, both the PEUU and PEUU-Tac sheets remained intact after 14 days, similar to our *in vitro* degradation studies, as well as previous studies using PEUU matrices in other rodent models (Takanari et al., 2016; D'amore et al., 2016). The PEUU-Tac matrices were easily removed after 14 days (Fig. 5c) with obvious growth of new muscular and connective tissues. In these studies, we

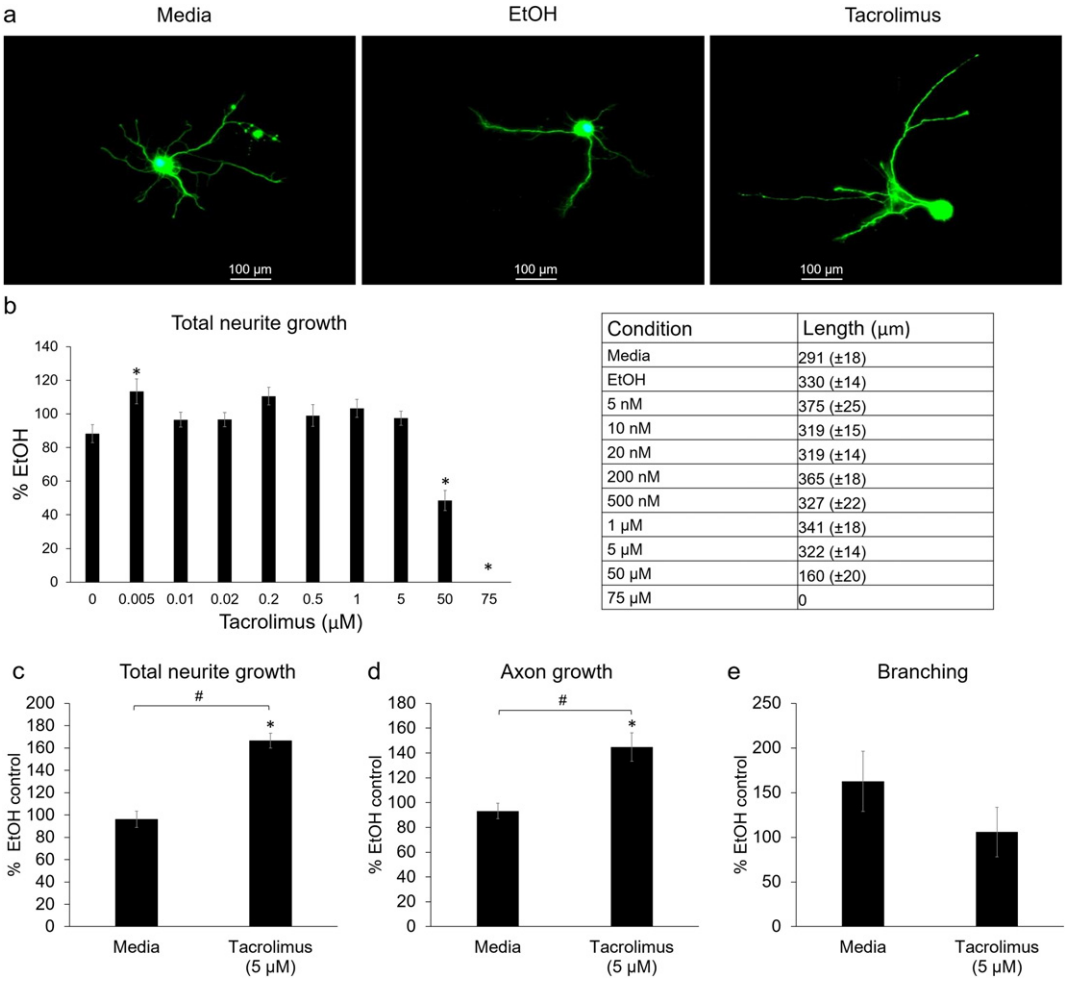

Condition	Length (μm)
Media	291 (±18)
EtOH	330 (±14)
5 nM	375 (±25)
10 nM	319 (±15)
20 nM	319 (±14)
200 nM	365 (±18)
500 nM	327 (±22)
1 μM	341 (±18)
5 μM	322 (±14)
50 μM	160 (±20)
75 μM	0

Fig. 2. a. Representative RGC images in media, EtOH (0.025%) vehicle, and tacrolimus (5 nM). b. Total neurite growth was greatest at 5 nM, but did not follow a typical dose response curve in high density cultures over the concentration range tested. However, at concentrations over 5 μM, total neurite growth decreased similarly to viability, reaching zero at 75 μM. The actual total neurite growth values for the data in graph b are indicated in the table. c–e. In low density cultures, analysis of neurite growth from non-contacting RGCs revealed distinct tacrolimus-dependent changes in neurite growth. For these experiments, we used 5 μM, the highest concentration that supported 100% viability and robust neurite growth. c. At 5 μM, total neurite growth in media was similar to vehicle at 96%. In contrast, tacrolimus treated neurons had 66% greater total neurite growth compared vehicle. d. Analysis of the longest neurite, the presumptive axon, showed the longest neurite in media was similar to vehicle at 93%. In contrast, tacrolimus increased axon growth by 45%. e. Branching remained unchanged with or without tacrolimus. b–e. Error bars represent the SEM. b. n ≥ 150 randomly analyzed neurons from triplicate cultures per experiment for at least 3 experimental repeats. c-d. n ≥ 30 neurons from triplicate wells for each of 3 experimental repeats, totaling ≥90 neurons per condition. $^{*}p < 0.05$

did not observe obvious cellular toxicity, necrosis, abnormal growth, nor inflammation in the ONs, which exhibited typical gross anatomical organization (Fig. 5d).

3.8. PEUU-Tac Delivered Tacrolimus Trans-durally to the Optic Nerve

Tacrolimus concentrations were analyzed in the blood, the retinas, and the ONs at 24 h and at 14 days post injury. At 24 h, PEUU-Tac increased tacrolimus in both fenestrated and unfenestrated ONs, but to significantly different extents (Fig. 6a–b). In fenestrated ONs, PEUU-Tac increased tacrolimus to approximately 56,000 ± 4319 ng/g. In these animals, tacrolimus was also detected in the ipsilateral retina but at a much lower concentration, 1500 ± 898 ng/g, as well as in the contralateral retina, at 438 ± 31 ng/g, and ON, at 569 ± 64 ng/g (Fig. 6a). In unfenestrated nerves, PEUU-Tac increased tacrolimus to approximately 5000 ± 1246 ng/g, approximately 11-fold lower than in fenestrated ONs. Similarly, tacrolimus also increased tacrolimus in the ipsilateral retina to 1900 ± 1484 μg/g, which was not significantly different than the ON. Moreover, tacrolimus was also detected in the contralateral retina at 341 ± 44 ng/g and ON at 1700 ± 225 ng/g.

In PEUU-Tac treated ONs, tacrolimus persisted over the 14-day time point analyzed. Despite the rapid release kinetics measured *in vitro*, tacrolimus remained detectable in PEUU-Tac treated ONs at levels similar to animals treated with tacrolimus systemically. At 14 days, tacrolimus was measured at 3300 ± 1151 ng/g in the PEUU-Tac treated ONs and at 609 ± 144 ng/g in the ipsilateral retina. In the contralateral ON, tacrolimus was measured at 2200 ± 477 ng/g and at 559 ± 100 ng/g in the contralateral retina. Thus, in the unfenestrated ONs, tacrolimus levels were increased in the right ON compared to both retinas but not the contralateral ON. Interestingly, systemic injections of tacrolimus at 2.2 mg/kg/day increased tacrolimus similarly in both ONs and in both retinas, but at significantly lower levels than their accompanying ON. Tacrolimus was measured at 2200 ± 304 ng/g in the right ON and at 1700 ± 175 ng/g in the left ON, and at 530 ± 44 ng/g in the right retina and at 618 ± 60 ng/g in the left retina. Interestingly, tacrolimus levels in both the ONs and in the retinas were similar to the ONs and the retinas in the PEUU-Tac treated animals at 14 days post implantation (Fig. 6c–d). Though further study is required, these data suggest PEUU-Tac applied to one ON delivers tacrolimus trans-durally to the treated ON and contiguous ocular tissues as effectively as daily systemic injections.

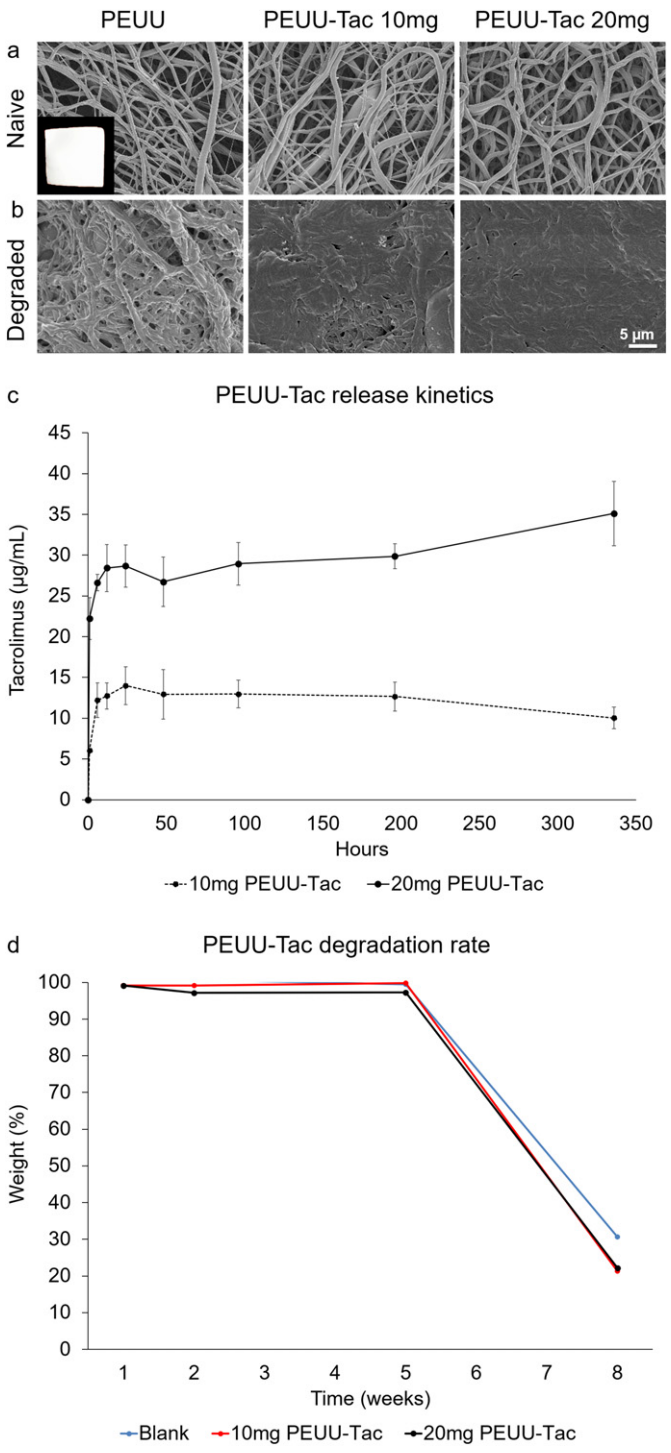

Fig. 3. Macro- and microscopic PEUU and PEUU-Tac morphologies, tacrolimus release kinetics, and degradation rates. a. Initial microscopic polymer size and organization in PEUU and 10 and 20 mg PEUU-Tac matrices. Inset shows typical macroscopic appearance for all three matrices. b. Microscopic organization in PEUU and 10 or 20 mg PEUU-Tac after 8 weeks of degradation in PBS. Note the almost complete absence of identifiable polymers in the PEUU-Tac matrices. c. Both 10 and 20 mg PEUU-Tac released tacrolimus rapidly and maximally by 24 h yielding concentrations of approximately 9.5 µg/ml and 23.7 µg/ml respectively. In both the 10 mg and 20 mg PEUU-Tac matrices, there were detectable changes in tacrolimus concentration. d. Based on weight and despite tacrolimus released, PEUU and 10 mg and 20 mg PEUU-Tac degraded similarly by weight in PBS at 37 °C, pH 7.4. All three matrices significantly decreased in weight between 5 and 8 weeks. a. Scale bar is 5 µm. c–d. n = 3 per experiment for three experimental repeats. Error bars in c indicate the SEM, and I error bars in d indicate SD.

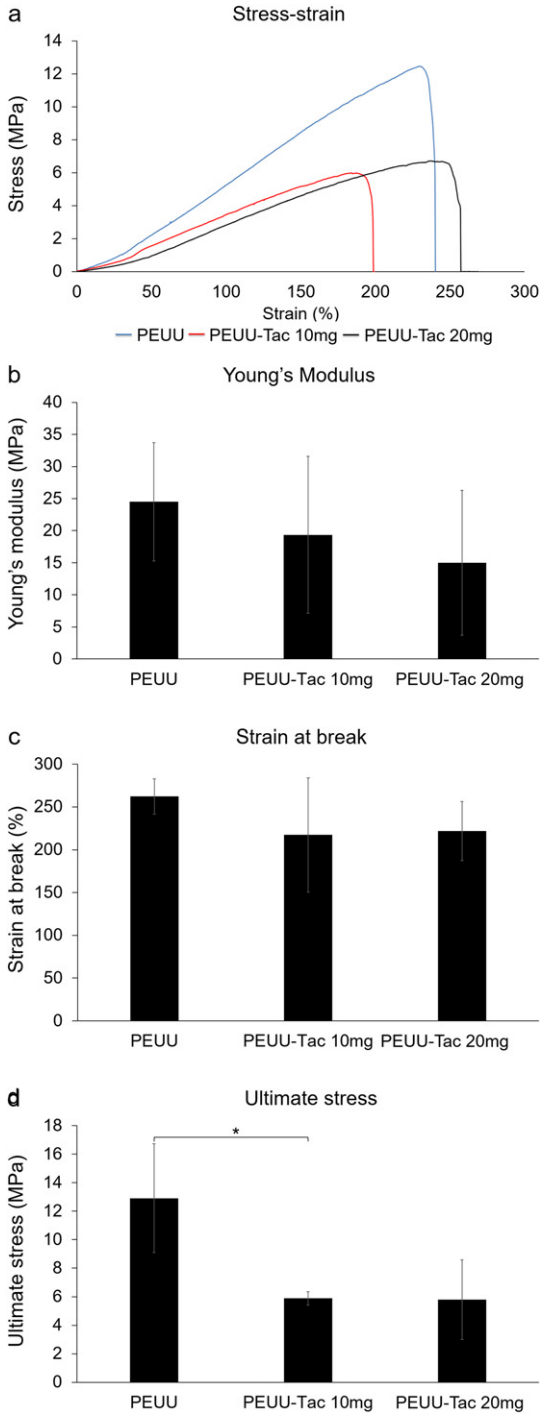

Fig. 4. Mechanical properties of PEUU and PEUU-Tac matrices. a. The stress-strain response is shown for PEUU and 10 and 20 mg PEUU-Tac. b. PEUU and PEUU-Tac matrices had similar Young's moduli and c. strains at break. d. Compared to PEUU, 10 mg PEUU-Tac had a significantly lower ultimate stress. Data represent triplicates per experiment for three experimental repeats. Error bars indicate the SD. $^{*}p < 0.05$.

3.9. PEUU-Tac Fails to Increase Tacrolimus Blood Levels Significantly

Compared to systemic administration, tacrolimus blood levels in PEUU-Tac treated animals were significantly lower (Fig. 6e–g). At 24 h, tacrolimus blood concentrations were below detection. At 14 days, tacrolimus was detected at 0.15 ± 0.05 ng/ml, which is well below typical therapeutic trough levels, which typically range from 10 to 20 ng/ml. In contrast, systemically administered tacrolimus

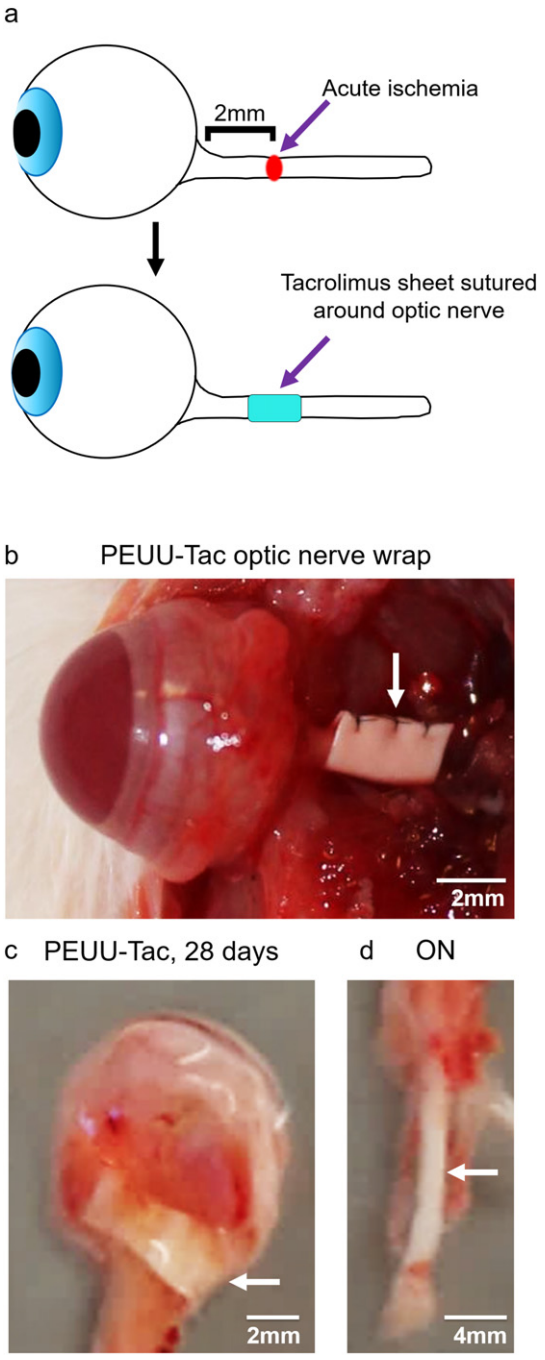

Fig. 5. Surgical approach to use PEUU-Tac to treat acute optic nerve (ON) ischemia. a. Acute ischemia model. To induce acute ischemia, a Yasargil aneurism clip was clamped on the ON approx. 2 mm behind the globe for 10s. Immediately after injury, a 2 mm × 5 mm PEUU-Tac matrix was wrapped around the nerve and sutured to itself and to the nerve sheath. b. In a euthanized animal the ON was completely exposed to more clearly show how PEUU-Tac was positioned and sutured. c. Over 14 days *in vivo*, PEUU-Tac matrices were clearly visible and easily removed. Note, by 14 days the sutures had dissolved and new connective and muscle tissues were clearly growing around the ON and under the PEUU-Tac matrix. Arrow indicates the PEUU-Tac matrix. d. Image of a typical ON after 14 days. In this study, no overt signs of necrosis or inflammation were observed in any of the animals. Arrow indicates typical ON morphology observed for both injured and uninjured nerves.

blood levels were measured at 7 ± 1 ng/ml at 24 h and 28 ± 4 ng/ml at 14 days, above typical therapeutic trough levels. Thus, despite similar tacrolimus concentrations in the ONs and in the retinas, tacrolimus blood levels were significantly reduced in PEUU-Tac treated animals, suggesting tacrolimus selectively accumulates in both the retinas and to a greater degree in the ONs irrespective of the administration route based on the 10 mg PEUU-Tac and systemic concentrations (2.2 mg/kg/day) used in this study.

3.10. After Acute ON Ischemia, PEUU-Tac Downregulates GFAP Expression

To determine if PEUU-Tac delivers bioactive tacrolimus trans-durally to glial cells, we analyzed *GFAP* expression, a marker for astrocyte activation, at the injury site (Fig. 7). Compared to sham, uninjured nerves, *GFAP* expression increased significantly at the injury site in ONs after acute ischemia, consistent with typical astrocyte *GFAP* expression, migration, and proliferation responses to acute ON injury (Fig. 7a–b). Qualitatively, increased magnification images showed obvious increases in *GFAP* expression at the injury site compared to uninjured nerves. *GFAP* was also increased in injured nerves treated with PEUU-Tac wraps or systemic tacrolimus but to a lesser extent (Fig. 7c–f). Quantitatively, *GFAP* expression increased significantly in injured ONs, but not ONs wrapped in PEUU-Tac or treated systemically with tacrolimus (Fig. 7g), consistent with previous systemic tacrolimus studies (Fields et al., 2016).

3.11. After Acute ON Ischemia, PEUU-Tac Increases GAP-43 Expression

To determine if PEUU-Tac delivers bioactive tacrolimus that can promote RGC axon survival or growth, we asked if PEUU-Tac increased the expression of the axon growth marker *GAP-43* (Fig. 8). Compared to injured nerves, PEUU-Tac increased *GAP-43* expression dramatically along the length of the ON (Fig. 8a–b). High magnification images of the injury site showed qualitatively that both PEUU-Tac and systemic tacrolimus increased *GAP-43* expression compared to injured, untreated nerves (Fig. 8c–f), consistent with previous studies analyzing the effects of systemic tacrolimus on CNS axons after acute ischemic CNS injury (Madsen et al., 1998; Rosenstiel et al., 2003). However, quantitatively, PEUU-Tac, but not systemic tacrolimus, increased *GAP-43* expression significantly in the ON (Fig. 8g). Though more detailed cellular analyses are warranted, these results demonstrate feasibility by showing that PEUU-Tac can deliver bioactive tacrolimus trans-durally to the ON to positively effect cellular markers indicative of a more positive tissue remodeling response to injury in the CNS.

4. Discussion

This study shows PEUU-Tac matrices, manufactured by electrospinning blended PEUU and tacrolimus, can be used to locally deliver bioactive tacrolimus trans-durally to CNS tissues without significantly raising blood levels. Tacrolimus is a macrolide calcineurin inhibitor often used as an immunosuppressant after allogeneic organ transplantation. In solid organ transplantation, life-long systemic tacrolimus immunosuppression is typically required to prevent rejection. Tacrolimus also has desirable neuroprotective and neuroregenerative properties for treating peripheral nerve or CNS injury and disease. However, treating nervous system tissues with systemic tacrolimus is complicated by the pharmacokinetic properties of tacrolimus. Tacrolimus is highly lipophilic and thus accumulates in fatty tissues throughout the body, including the myelin-based white matter in the CNS. However, for reasons not completely understood, higher systemic tacrolimus concentrations are necessary to effectively increase tacrolimus levels in CNS tissues. Due to the narrow therapeutic window for tacrolimus, systemic increases are not feasible since they would likely lead to toxic secondary exposures and potentially life-threatening side effects in non-targeted tissues or organs. Fortunately, pre-clinical models of acute ischemic nervous system injury indicate shorter therapeutic time windows are more effective in promoting positive CNS tissue remodeling, like increased axon growth (Yang et al., 2003; Madsen et al., 1998; Voda et al., 2005). These shorter therapeutic windows are in agreement with early modulation of the pro-inflammatory innate immune response and preventing or suppressing injury-induced

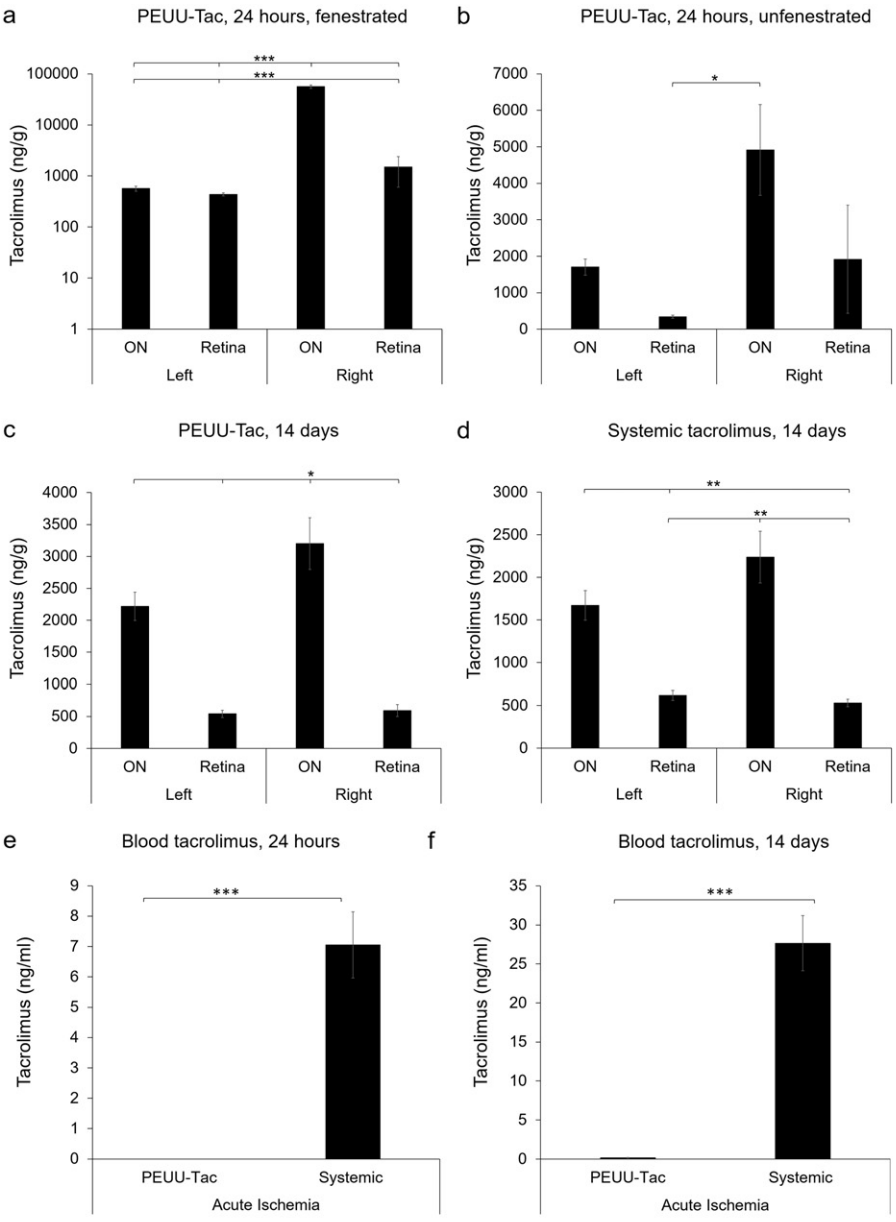

g

Group	24 hours	14 days
PEUU-Tac ON wrap	Below detection	0.15 (± 0.05) ng/ml
Systemic	7 (± 1) ng/ml	28 (± 4) ng/ml

Fig. 6. a–g. Tacrolimus concentrations in the optic nerves (ONs), in the retinas, and in the blood. a. In injured, fenestrated ON at 24 h, PEUU-Tac increased tacrolimus in the PEUU-Tac wrapped ON significantly to approximately 56,000 ng/g and in the ipsilateral retina to 1501 ng/g, as well as in the contralateral ON (569 ng/g) and retina (438 ng/g). b. In injured, unfenestrated ON at 24 h, PEUU-Tac increased tacrolimus in the PEUU-Tac wrapped ON to 4914 ng/g and in the ipsilateral retina to 1914 ng/g, as well as in the contralateral ON (1700 ng/g) and retina (341 ng/g). c. At 14 days, PEUU-Tac tacrolimus in the PEUU-Tac wrapped ON was measured at 3201 ng/g and in the ipsilateral retina at 592 ng/g. Tacrolimus also remained elevated in the contralateral ON (2219 ng/g) and retina (541 ng/g). d. After systemic administration, tacrolimus was elevated in both ONs and retinas. The tacrolimus levels in the left ON was 1671 ng/g and 619 ng/g in the left retina similar to tacrolimus in the right ON measured at 2238 ng/g and retina measured at 530 ng/g. e. At 24 h, tacrolimus was undetectable in the blood in PEUU-Tac treated animals, whereas tacrolimus in systemically treated animals was significantly higher at 7 (±1) ng/ml. At 14 days, tacrolimus increased to 0.15 ± 0.05 ng/ml in PEUU-Tac treated animals. In contrast, tacrolimus increased to 28 ± 4 ng/ml in systemically treated animals. N = 5 animals per group. Significance was determined by one-way ANOVA with Posthoc Tukey's test between groups. $^{*}p < 0.05$.

microglial and astrocyte activation (Wakita et al., 1998), which can increase CNS neuron survival (Liddelow et al., 2017) and decrease cellular and ECM remodeling preceding scar tissue formation (van der Merwe and Steketee, 2016). Modulating the early innate immune response has been shown to be a critical factor in vertebrates that can functionally regenerate CNS tissues (Godwin et al., 2013). Thus, the PEUU-Tac matrix reported here may fill a clinical need by providing a platform combining two FDA approved materials, into a tunable platform that can be secured in place to effectively deliver tacrolimus trans-durally to CNS tissues. Moreover, PEUU can be easily tuned with additional genetic and biochemical reagents tailored to the nature and the scope of the injury.

PEUU-Tac has desirable mechanical and biocompatible properties for treating CNS tissues. Like PEUU (Stankus et al., 2004), PEUU-Tac is a flexible, biodegradable polymeric matrix that can be easily cut, shaped, and sutured to the dura mater with mechanical and degradation properties that can be easily tuned to match the tissue of interest. In this study, PEUU-Tac's mechanical properties closely matched

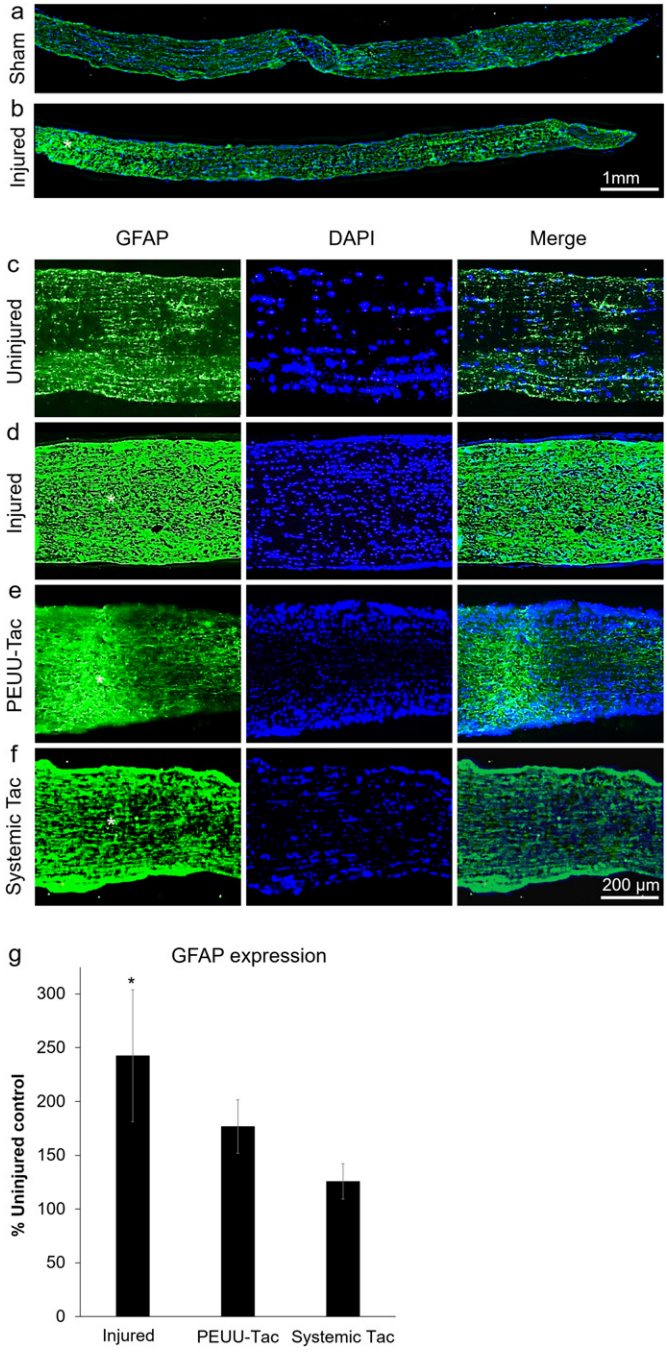

Fig. 7. PEUU-Tac decreases GFAP expression at the injury site. a. Representative full length optic nerves (ONs) showing GFAP expression at 14 days in a. a sham and b. in an injured ON after acute ischemia. c–f. Qualitatively, GFAP expression (green) is shown approx. 2 mm (*) behind the globe in c. an uninjured sham, d. an injured, untreated ON, e. an injured PEUU-Tac wrapped ON, and f. an injured animal treated with systemic tacrolimus (Systemic Tac). g. Quantitatively, GFAP expression increased significantly in injured ONs but not in ONs treated by PEUU-Tac or systemic tacrolimus. n ≥ 4 per condition at 14 days. Error bars represent the SEM. Significance was determined by one-way ANOVA with Post-hoc Tukey's test between groups. *$p < 0.05$.

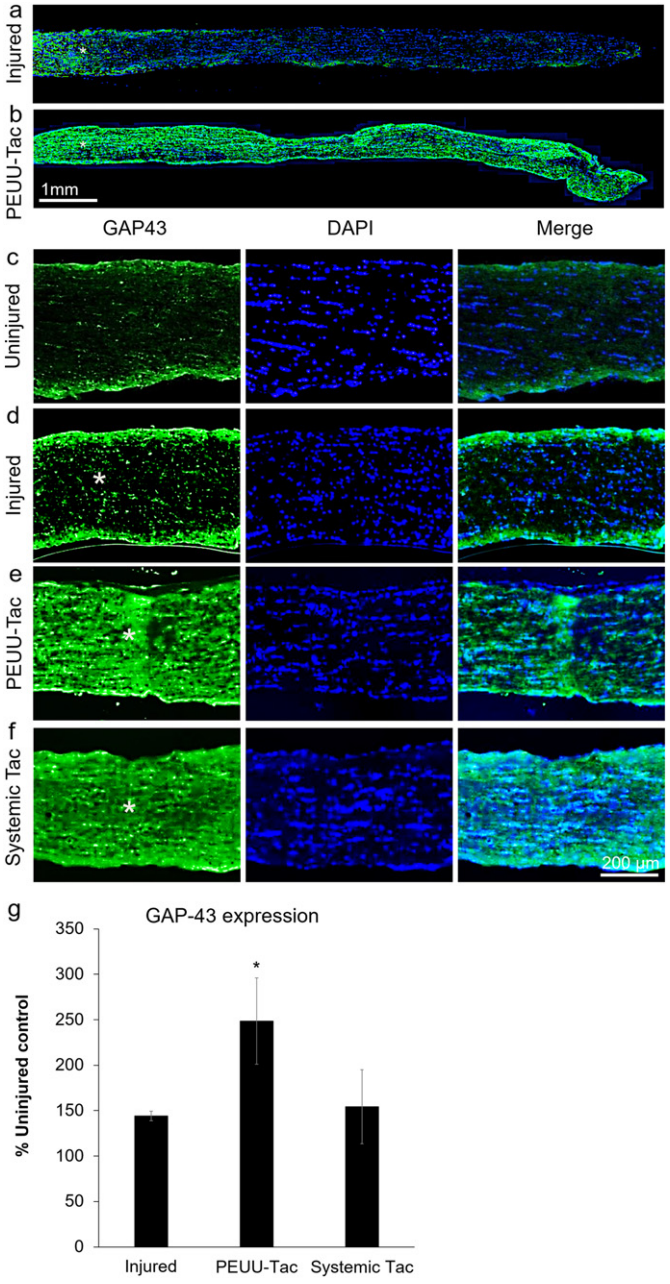

Fig. 8. PEUU-Tac increases GAP-43 expression. a. Representative full length optic nerves (ONs) showing GAP-43 expression at 14 days in a. an injured nerve and b. an injured nerve treated with PEUU-Tac c–f. Qualitatively, GAP-43 expression (green) is shown approx. 2 mm (*) behind the globe in c. an uninjured sham ON, d. an injured untreated ON, e. an injured PEUU-Tac wrapped ON, and f. an injured nerve treated systemically with tacrolimus (Systemic Tac). g. Quantitatively, GAP-43 expression increased significantly in PEUU-Tac treated ONs. n ≥ 4 per condition at 14 days. Error bars represent the SEM. Significance was determined by one-way ANOVA with Post-hoc Tukey's test between groups. *$p < 0.05$.

the biomechanical properties of the dura mater surrounding the CNS in both rodents and in humans. Matching biomechanics is necessary to effectively sustain physiologically applied mechanical forces (Griffin et al., 2016). In fact, PEUU was chosen specifically for this reason since PEUU polymers can be easily tuned to match the biomechanical properties of different tissues of interest (Stankus et al., 2004; Hong et al., 2011). In this study, PEUU-Tac matrices had breaking strains around 200% and tensile strengths around 6 MPa. In rat, the tensile strength for rat dura mater is generally reported to be under 3 MPA with breaking strains around 140% (Maikos et al., 2008; Fiford and Bilston, 2005) and, similarly, tensile strengths for human dura mater have been reported to be approximately 1–5 MPa with breaking strains considerably lower than PEUU (van Noort et al., 1981; Bilston and Thibault, 1996; Raykin et al., 2017). Thus, the PEUU-Tac matrices appear to be a good match biomechanically for trans-dural drug delivery to CNS tissues.

In vitro, PEUU-Tac released tacrolimus rapidly, approx. 85% was released within 24 h, resulting in a local concentration of 9.53 μg/ml or 11.3 μM for the 10 mg PEUU-Tac used in *in vivo* studies. After acute ON ischemia in rat, an ophthalmic surgeon surgically inserted PEUU-Tac through a narrow, almost bloodless conjunctival plane, wrapped the PEUU-Tac around the ON at the injury site by looping a suture connected to the wrap around the ON. The PEUU matrix was then sutured both to itself and to the dura to prevent movement. Like PEUU, PEUU-Tac exhibited good tolerance *in vivo* and possessed good suture retention. Obvious cellular toxicity, necrosis, abnormal growth, or inflammation were unobserved. After 2 weeks *in vivo*, PEUU-Tac matrices appeared intact and were easily removed, suggesting that if necessary, the matrices could have been removed earlier since tacrolimus release from PEUU-Tac was essentially complete within 24 h. Moreover, PEUU matrices could be replaced if needed with the same or different matrices to treat different phases of the default healing response in the CNS (Fitzgerald et al., 2010). Finally, the ability of a trained surgeon to perform this procedure in a rodent model is encouraging for treating ONs in humans, which provide easier access and greater exposure, but also for treating spinal cord, brain, and peripheral nerve injuries where biomechanical tissue compliance during flexion and/or suturing are desired.

PEUU-Tac delivered tacrolimus to ONs trans-durally without significantly increasing blood levels. In fenestrated ONs, tacrolimus increased to 56,000 ng/g, or approximately 70 μM, well above the toxicity limit (LD_{50} = 24 μM) measured for primary RGCs *in vitro* and above levels considered safe clinically which are typically in the low ng/g range. In unfenestrated nerves, PEUU-Tac also successfully increased tacrolimus but to levels 10-fold lower at 5000 ng/g or approximately 6 μM within 24 h. In PEUU-Tac treated ONs, tacrolimus remained detectable at 14 days, at around 3200 ng/g or 3.8 μM, which is still well above clinically accepted levels. Moreover, these concentrations are several hundred fold higher than blood trough concentrations (>10–30 ng/ml or 10–30 nM) shown to be neurotoxic in the CNS (Toledo Perdomo et al., 2012; Bechstein, 2000) and in the PNS (Arnold et al., 2013). Tacrolimus was also detected in the contralateral ON (2200 ng/g, 2.6 μM) and at lower levels in both the ipsilateral (591 ng/g, 0.7 μM) and contralateral (541 ng/g, 0.66 μM) retinas, indicating contiguous ocular tissues also absorbed tacrolimus. However, despite high ON levels and detection in other ocular tissues, tacrolimus was undetectable in the blood at 24 h and minimally detected at 0.15 ± 0.05 ng/ml after 14 days compared to systemic tacrolimus blood levels measured at 27.66 ± 3.53 ng/ml after 14 days. These results indicate PEUU-Tac can deliver tacrolimus trans-durally to CNS tissues, However, the initial tacrolimus concentration measured in this study are too high, requiring either lower initial tacrolimus concentrations in the PEUU-Tac matrix and/or slower release kinetics, both properties that are easily modified and expected to further reduce absorption by adjacent ocular tissues and by the blood. Using data from this study and physiologically based pharmacokinetics, studies are ongoing to determine the appropriate tacrolimus loading concentrations and release kinetics from PEUU-Tac to maximize the cellular responses to acute ischemic injury and to minimize neurotoxicity.

After acute ON ischemia, PEUU-Tac positively modulated typical markers of the default healing response in CNS tissues. After ON injury, injured RGC axons typically degenerate (Benowitz et al., 2017) and astrocytes, among other immune and glial cells, proliferate and migrate to the injury site, locally increasing *GFAP* expression and contributing to scar tissue formation (Silver and Miller, 2004). In PEUU-Tac wrapped nerves, *GFAP* expression increased but to significantly lower levels at the injury site than in untreated, injured ONs. Moreover, in PEUU-Tac treated nerves *GAP-43* expression increased along the length of the ON, similar to observations after systemic tacrolimus delivery (Madsen et al., 1998; Rosenstiel et al., 2003). Though additional cellular and functional studies are required, these initial data show that, despite the high tacrolimus ON concentrations measured, PEUU-Tac delivers bioactive tacrolimus trans-durally that is sufficient to decrease *GFAP* expression and presumably astrogliosis, while increasing *GAP-43* expression and presumably RGC axon growth. Once tacrolimus loading and/or release kinetics are optimized for the PEUU-Tac matrices, future studies will include functional studies to correlate axon growth and decreased astrocyte activation with neuronal signaling and visual function.

Though these initial studies demonstrate feasibility, several caveats need to be addressed for optimizing PEUU-Tac for functional studies. FKBPs are enriched in CNS tissues (Lyson et al., 1993) and tacrolimus is highly lipophilic, suggesting tacrolimus may selectively accumulate in CNS tissues with high myelin content, like the ON. Though oligodendrocytes may not express FKBP (Kato et al., 2000), tacrolimus influences myelination (Gold et al., 2004) and oligodendrocyte survival *in vitro* (Craighead et al., 1999; Nottingham et al., 2002). Second, different FKBP receptors are differentially expressed by CNS neurons like RGCs (Freeman and Grosskreutz, 2000) and many glial cells, resulting in varying regulation of different signaling pathways involved in cell cycle control (Aghdasi et al., 2001), neuronal motility (Ahearn et al., 2011), and apoptosis (Anghel et al., 2013), highlighting the importance of analyzing the inter- and intracellular effects of tacrolimus within CNS cellular populations. Third, tacrolimus has also been shown to effect blood brain barrier integrity and function (Anghel et al., 2013) and thus may differentially regulate absorption, particularly at local delivery sites where tacrolimus concentrations are high. Regulating tacrolimus tissue and blood levels is critical due to the narrow therapeutic index, tissue absorption variability, and pharmokinetic variability, (Jacobson et al., 2001) and thus is further complicated by the number of cellular targets and compartmentalization. Hence, bioavailability of tacrolimus differs across cellular populations. Whether the measured tacrolimus concentration in the ON in this study accurately reflects tacrolimus bioavailability is unknown, but this information is required to properly tune PEUU-Tac matrices for dosing. Clinically, tacrolimus doses are based on whole blood trough levels, which poorly predict tissue levels; even within the therapeutic range, toxicity may occur (Sikma et al., 2015). Furthermore, physiology, age, and concurrent medications can alter tacrolimus levels and biological activity (Diehl et al., 2017). Thus, tacrolimus tissue concentrations at target sites may better predict outcomes (Noll et al., 2013), highlighting the need to optimize tacrolimus delivery time and concentration indices for CNS tissues specifically prior to conducting functional studies.

5. Conclusion

Injury to CNS tissues like the ON often leads to a pro-inflammatory innate immune response, negative tissue remodeling to form scar tissue, and axon degeneration that leads to permanently lost neurological function. The PEUU-Tac matrix proposed here utilizes cost effective materials already used in FDA approved products. These materials are readily available, do not produce adverse immune responses when used correctly, and are highly translatable clinically. The combination of the two materials provides a device capable of being tailored to a patient's specific injury, increasing the probability of a positive outcome. Clinically, tacrolimus has a narrow therapeutic index and high inter- and intra-individual pharmacokinetic variability, necessitating therapeutic drug monitoring to individualize dosage. The sustained detection of tacrolimus in the ON and positive effects on tissue remodeling indicate that a single PEUU-Tac application may be sufficient to treat ON injury where systemic administration requires frequent injections to maintain the same tacrolimus levels. Thus, PEUU-Tac could greatly reduce issues with patient compliance/adherence to the treatment and decrease the chances of unwanted, potentially life-threatening side-effects (Bottiger et al., 1999; Randhawa et al., 1997; Mayer et al., 1997).

Acknowledgments

We thank Donna Stoltz and the Center for Biologic Imaging at the University of Pittsburgh for expertise in scanning electron microscopy and Lori Walton and the Histology Core at the McGowan Institute for tissue processing.

Funding Sources

We gratefully acknowledge funding from the Department of Defense, Office of Congressionally Directed Medical Research Programs and the Clinical and Rehabilitative Medicine Research Program (MBS, W81XWH-15-1-0026), Pennsylvania Lions Sight Conservation & Eye Research Foundation (MBS), Start-up funds, NIH CORE Grant P30 EY08098 to the Department of Ophthalmology, from the Eye and Ear Foundation of Pittsburgh, and from an unrestricted grant from Research to Prevent Blindness, New York, NY.

Conflict of Interest

The authors declare no competing financial interests.

Author Contributions

Experimental design: Y. vdM., I.C., X.G., V. S. G., R. V., K.M.W., W.R.W., M.B.S.

Conduct experiments: Y. vdM., A.E.F., I.C., X.G., F.F., W.Z., B. L., S. R.

Data analysis: Y. vdM., A.E.F., X.G., F.F., W.Z., B. L., S. R., R. V., M.B.S.

Manuscript writing: Y. vdM., X.G., F.F., V. S. G., R. V., W.R.W., M.B.S.

References

Aghdasi, B., Ye, K., Resnick, A., Huang, A., Ha, H.C., Guo, X., Dawson, T.M., Dawson, V.L., Snyder, S.H., 2001. FKBP12, the 12-kDa FK506-binding protein, is a physiologic regulator of the cell cycle. Proc. Natl. Acad. Sci. U. S. A. 98, 2425–2430.

Ahearn, I.M., Tsai, F.D., Court, H., Zhou, M., Jennings, B.C., Ahmed, M., Fehrenbacher, N., Linder, M.E., Philips, M.R., 2011. FKBP12 binds to acylated H-ras and promotes depalmitoylation. Mol. Cell 41, 173–185.

Anghel, D., Tanasescu, R., Campeanu, A., Lupescu, I., Podda, G., Bajenaru, O., 2013. Neurotoxicity of immunosuppressive therapies in organ transplantation. Maedica (Buchar) 8, 170–175.

Arnold, R., Pussell, B.A., Pianta, T.J., Lin, C.S., Kiernan, M.C., Krishnan, A.V., 2013. Association between calcineurin inhibitor treatment and peripheral nerve dysfunction in renal transplant recipients. Am. J. Transplant. 13, 2426–2432.

Barres, B.A., Silverstein, B.E., Corey, D.P., Chun, L.L., 1988. Immunological, morphological, and electrophysiological variation among retinal ganglion cells purified by panning. Neuron 1, 791–803.

Bechstein, W.O., 2000. Neurotoxicity of calcineurin inhibitors: impact and clinical management. Transpl. Int. 13, 313–326.

Benowitz, L.I., He, Z., Goldberg, J.L., 2017. Reaching the brain: advances in optic nerve regeneration. Exp. Neurol. 287, 365–373.

Bilston, L.E., Thibault, L.E., 1996. The mechanical properties of the human cervical spinal cord in vitro. Ann. Biomed. Eng. 24, 67–74.

Bottiger, Y., Brattstrom, C., Tyden, G., Sawe, J., Groth, C.G., 1999. Tacrolimus whole blood concentrations correlate closely to side-effects in renal transplant recipients. Br. J. Clin. Pharmacol. 48, 445–448.

Chen, B., Wu, Q., Ke, G., Bu, B., 2017. Efficacy and safety of tacrolimus treatment for neuromyelitis optica spectrum disorder. Sci. Rep. 7, 831.

Craighead, M.W., Tiwari, P., Keynes, R.G., Waters, C.M., 1999. Human oligodendroglial cell line, MO3.13, can be protected from apoptosis using the general caspase inhibitor zVAD-FMK. J. Neurosci. Res. 57 (2), 236–243.

D'amore, A., Yoshizumi, T., Luketich, S.K., Wolf, M.T., Gu, X., Cammarata, M., Hoff, R., Badylak, S.F., Wagner, W.R., 2016. Bi-layered polyurethane - extracellular matrix cardiac patch improves ischemic ventricular wall remodeling in a rat model. Biomaterials 107, 1–14.

Deuse, T., Blankenberg, F., Haddad, M., Reichenspurner, H., Phillips, N., Robbins, R.C., Schrepfer, S., 2010. Mechanisms behind local immunosuppression using inhaled tacrolimus in preclinical models of lung transplantation. Am. J. Respir. Cell Mol. Biol. 43, 403–412.

Diehl, R., Ferrara, F., Muller, C., Dreyer, A.Y., Mcleod, D.D., Fricke, S., Boltze, J., 2017. Immunosuppression for in vivo research: state-of-the-art protocols and experimental approaches. Cell Mol. Immunol. 14, 146–179.

Faust, A., Kandakatla, A., Van Der Merwe, Y., Ren, T., Huleihel, L., Hussey, G., Naranjo, J.D., Johnson, S., Badylak, S., Steketee, M., 2017. Urinary bladder extracellular matrix hydrogels and matrix-bound vesicles differentially regulate central nervous system neuron viability and axon growth and branching. J. Biomater. Appl. 31, 1277–1295.

Fields, J.A., Overk, C., Adame, A., Florio, J., Mante, M., Pineda, A., Desplats, P., Rockenstein, E., Achim, C., Masliah, E., 2016. Neuroprotective effects of the immunomodulatory drug FK506 in a model of HIV1-gp120 neurotoxicity. J. Neuroinflammation 13, 120.

Fiford, R.J., Bilston, L.E., 2005. The mechanical properties of rat spinal cord in vitro. J. Biomech. 38, 1509–1515.

Fitzgerald, M., Bartlett, C.A., Harvey, A.R., Dunlop, S.A., 2010. Early events of secondary degeneration after partial optic nerve transection: an immunohistochemical study. J. Neurotrauma 27, 439–452.

Freeman, E.E., Grosskreutz, C.L., 2000. The effects of FK506 on retinal ganglion cells after optic nerve crush. Invest. Ophthalmol. Vis. Sci. 41, 1111–1115.

Fukuta, T., Ishii, T., Asai, T., Sato, A., Kikuchi, T., Shimizu, K., Minamino, T., Oku, N., 2015. Treatment of stroke with liposomal neuroprotective agents under cerebral ischemia conditions. Eur. J. Pharm. Biopharm. 97, 1–7.

Gabriel, D., Mugnier, T., Courthion, H., Kranidioti, K., Karagianni, N., Denis, M.C., Lapteva, M., Kalia, Y., Moller, M., Gurny, R., 2016. Improved topical delivery of tacrolimus: a novel composite hydrogel formulation for the treatment of psoriasis. J. Control. Release 242, 16–24.

Godwin, J.W., Pinto, A.R., Rosenthal, N.A., 2013. Macrophages are required for adult salamander limb regeneration. Proc. Natl. Acad. Sci. U. S. A. 110, 9415–9420.

Gold, B.G., Voda, J., Yu, X., McKeon, G., Bourdette, D.N., 2004. FK506 and a nonimmunosuppressant derivative reduce axonal and myelin damage in experimental autoimmune encephalomyelitis: neuroimmunophilin ligand-mediated neuroprotection in a model of multiple sclerosis. J. Neurosci. Res. 77 (3), 367–377.

Gold, B.G., Armistead, D.M., Wang, M.S., 2005. Non-FK506-binding protein-12 neuroimmunophilin ligands increase neurite elongation and accelerate nerve regeneration. J. Neurosci. Res. 80, 56–65.

Griffin, M., Premakumar, Y., Seifalian, A., Butler, P.E., Szarko, M., 2016. Biomechanical characterization of human soft tissues using indentation and tensile testing. J. Vis. Exp. 118. https://doi.org/10.3791/54872.

Guan, J., Sacks, M.S., Beckman, E.J., Wagner, W.R., 2002. Synthesis, characterization, and cytocompatibility of elastomeric, biodegradable poly(ester-urethane)ureas based on poly(caprolactone) and putrescine. J. Biomed. Mater. Res. 61, 493–503.

Hong, Y., Guan, J., Fujimoto, K.L., Hashizume, R., Pelinescu, A.L., Wagner, W.R., 2010. Tailoring the degradation kinetics of poly(ester carbonate urethane)urea thermoplastic elastomers for tissue engineering scaffolds. Biomaterials 31, 4249–4258.

Hong, Y., Huber, A., Takanari, K., Amoroso, N.J., Hashizume, R., Badylak, S.F., Wagner, W.R., 2011. Mechanical properties and in vivo behavior of a biodegradable synthetic polymer microfiber-extracellular matrix hydrogel biohybrid scaffold. Biomaterials 32, 3387–3394.

Horn, K.P., Busch, S.A., Hawthorne, A.L., VAN Rooijen, N., Silver, J., 2008. Another barrier to regeneration in the CNS: activated macrophages induce extensive retraction of dystrophic axons through direct physical interactions. J. Neurosci. 28, 9330–9341.

Howrie, D.L., Ptachcinski, R.J., Griffith, B.P., Hardesty, R.J., Rosenthal, J.T., Burckart, G.J., Venkataramanan, R., 1985. Anaphylactoid reactions associated with parenteral cyclosporine use: possible role of Cremophor EL. Drug Intell. Clin. Pharm. 19, 425–427.

Jacobson, P., Ng, J., Ratanatharathorn, V., Uberti, J., Brundage, R.C., 2001. Factors affecting the pharmacokinetics of tacrolimus (FK506) in hematopoietic cell transplant (HCT) patients. Bone Marrow Transplant. 28, 753–758.

Kato, H., Oikawa, T., Otsuka, K., Takahashi, A., Itoyama, Y., 2000. Postischemic changes in the immunophilin FKBP12 in the rat brain. Brain Res. Mol. Brain Res. 84, 58–66.

Lapteva, M., Mondon, K., Moller, M., Gurny, R., Kalia, Y.N., 2014. Polymeric micelle nanocarriers for the cutaneous delivery of tacrolimus: a targeted approach for the treatment of psoriasis. Mol. Pharm. 11, 2989–3001.

Liddelow, S.A., Guttenplan, K.A., Clarke, L.E., Bennett, F.C., Bohlen, C.J., Schirmer, L., Bennett, M.L., Munch, A.E., Chung, W.S., Peterson, T.C., Wilton, D.K., Frouin, A., Napier, B.A., Panicker, N., Kumar, M., Buckwalter, M.S., Rowitch, D.H., Dawson, V.L., Dawson, T.M., Stevens, B., Barres, B.A., 2017. Neurotoxic reactive astrocytes are induced by activated microglia. Nature 541, 481–487.

Liu, W., Tang, Y., Feng, J., 2011. Cross talk between activation of microglia and astrocytes in pathological conditions in the central nervous system. Life Sci. 89, 141–146.

Lyson, T., Ermel, L.D., Belshaw, P.J., Alberg, D.G., Schreiber, S.L., Victor, R.G., 1993. Cyclosporine- and FK506-induced sympathetic activation correlates with calcineurin-mediated inhibition of T-cell signaling. Circ. Res. 73, 596–602.

Madan, V., Griffiths, C.E., 2007. Systemic ciclosporin and tacrolimus in dermatology. Dermatol. Ther. 20, 239–250.

Madsen, J.R., Macdonald, P., Irwin, N., Goldberg, D.E., Yao, G.L., Meiri, K.F., Rimm, I.J., Stieg, P.E., Benowitz, L.I., 1998. Tacrolimus (FK506) increases neuronal expression of GAP-43 and improves functional recovery after spinal cord injury in rats. Exp. Neurol. 154, 673–683.

Maikos, J.T., Elias, R.A., Shreiber, D.I., 2008. Mechanical properties of dura mater from the rat brain and spinal cord. J. Neurotrauma 25, 38–51.

Mayer, A.D., Dmitrewski, J., Squifflet, J.P., Besse, T., Grabensee, B., Klein, B., Eigler, F.W., Heemann, U., Pichlmayr, R., Behrend, M., Vanrenterghem, Y., Donck, J., VAN Hooff, J., Christiaans, M., Morales, J.M., Andres, A., Johnson, R.W., Short, C., Buchholz, B., Rehmert, N., Land, W., Schleibner, S., Forsythe, J.L., Talbot, D., Pohanka, E., et al., 1997. Multicenter randomized trial comparing tacrolimus (FK506) and cyclosporine in the prevention of renal allograft rejection: a report of the European Tacrolimus Multicenter Renal Study Group. Transplantation 64, 436–443.

Mccloy, R.A., Rogers, S., Caldon, C.E., Lorca, T., Castro, A., Burgess, A., 2014. Partial inhibition of Cdk1 in G 2 phase overrides the SAC and decouples mitotic events. Cell Cycle 13, 1400–1412.

Noll, B.D., Coller, J.K., Somogyi, A.A., Morris, R.G., Russ, G.R., Hesselink, D.A., VAN Gelder, T., Sallustio, B.C., 2013. Validation of an LC-MS/MS method to measure tacrolimus in rat kidney and liver tissue and its application to human kidney biopsies. Ther. Drug Monit. 35, 617–623.

Nottingham, S., Knapp, P., Springer, J., 2002. FK506 treatment inhibits caspase-3 activation and promotes oligodendroglial survival following traumatic spinal cord injury. Exp. Neurol. 177 (1), 242–251.
Peruzzotti-Jametti, L., Donega, M., Giusto, E., Mallucci, G., Marchetti, B., Pluchino, S., 2014. The role of the immune system in central nervous system plasticity after acute injury. Neuroscience 283, 210–221.
Petan, J.A., Undre, N., First, M.R., Saito, K., Ohara, T., Iwabe, O., Mimura, H., Suzuki, M., Kitamura, S., 2008. Physiochemical properties of generic formulations of tacrolimus in Mexico. Transplant. Proc. 40, 1439–1442.
Randhawa, P.S., Starzl, T.E., Demetris, A.J., 1997. Tacrolimus (FK506)-associated renal pathology. Adv. Anat. Pathol. 4, 265–276.
Raykin, J., Forte, T.E., Wang, R., Feola, A., Samuels, B.C., Myers, J.G., Mulugeta, L., Nelson, E.S., Gleason, R.L., Ethier, C.R., 2017. Characterization of the mechanical behavior of the optic nerve sheath and its role in spaceflight-induced ophthalmic changes. Biomech. Model. Mechanobiol. 16, 33–43.
Rosenstiel, P., Schramm, P., Isenmann, S., Brecht, S., Eickmeier, C., Burger, E., Herdegen, T., Sievers, J., Lucius, R., 2003. Differential effects of immunophilin-ligands (FK506 and V-10,367) on survival and regeneration of rat retinal ganglion cells in vitro and after optic nerve crush in vivo. J. Neurotrauma 20, 297–307.
Russo, R., Varano, G.P., Adornetto, A., Nucci, C., Corasaniti, M.T., Bagetta, G., Morrone, L.A., 2016. Retinal ganglion cell death in glaucoma: exploring the role of neuroinflammation. Eur. J. Pharmacol. 787, 134–142.
Sarikcioglu, L., Demir, N., Demirtop, A., 2007. A standardized method to create optic nerve crush: Yasargil aneurysm clip. Exp. Eye Res. 84, 373–377.
Sharifi, Z.N., Abolhassani, F., Zarrindast, M.R., Movassaghi, S., Rahimian, N., Hassanzadeh, G., 2012. Effects of FK506 on hippocampal CA1 cells following transient global ischemia/reperfusion in Wistar rat. Stroke Res. Treat. 2012, 809417.
Sikma, M.A., Van Maarseveen, E.M., Van De Graaf, E.A., Kirkels, J.H., Verhaar, M.C., Donker, D.W., Kesecioglu, J., Meulenbelt, J., 2015. Pharmacokinetics and toxicity of tacrolimus early after heart and lung transplantation. Am. J. Transplant. 15, 2301–2313.
Silver, J., Miller, J.H., 2004. Regeneration beyond the glial scar. Nat. Rev. Neurosci. 5, 146–156.
Solari, M.G., Washington, K.M., Sacks, J.M., Hautz, T., Unadkat, J.V., Horibe, E.K., Venkataramanan, R., Larregina, A.T., Thomson, A.W., Lee, W.P., 2009. Daily topical tacrolimus therapy prevents skin rejection in a rodent hind limb allograft model. Plast. Reconstr. Surg. 123, 17S–25S.
Stankus, J.J., Guan, J., Wagner, W.R., 2004. Fabrication of biodegradable elastomeric scaffolds with sub-micron morphologies. J. Biomed. Mater. Res. A 70, 603–614.
Starzl, T.E., Todo, S., Fung, J., Demetris, A.J., Venkataramman, R., Jain, A., 1989. FK 506 for liver, kidney, and pancreas transplantation. Lancet 2, 1000–1004.
Steketee, M.B., Tosney, K.W., 1999. Contact with isolated sclerotome cells steers sensory growth cones by altering distinct elements of extension. J. Neurosci. 19, 3495–3506.
Steketee, M.B., Moysidis, S.N., Jin, X.L., Weinstein, J.E., Pita-Thomas, W., Raju, H.B., Iqbal, S., Goldberg, J.L., 2011. Nanoparticle-mediated signaling endosome localization regulates growth cone motility and neurite growth. Proc. Natl. Acad. Sci. U. S. A. 108, 19042–19047.
Szydlowska, K., Zawadzka, M., Kaminska, B., 2006. Neuroprotectant FK506 inhibits glutamate-induced apoptosis of astrocytes in vitro and in vivo. J. Neurochem. 99, 965–975.
Tajdaran, K., Shoichet, M.S., Gordon, T., Borschel, G.H., 2015. A novel polymeric drug delivery system for localized and sustained release of tacrolimus (FK506). Biotechnol. Bioeng. 112, 1948–1953.
Takanari, K., Hong, Y., Hashizume, R., Huber, A., Amoroso, N.J., D'amore, A., Badylak, S.F., Wagner, W.R., 2016. Abdominal wall reconstruction by a regionally distinct biocomposite of extracellular matrix digest and a biodegradable elastomer. J. Tissue Eng. Regen. Med. 10, 748–761.
Tang, S., Qiu, J., Nikulina, E., Filbin, M.T., 2001. Soluble myelin-associated glycoprotein released from damaged white matter inhibits axonal regeneration. Mol. Cell. Neurosci. 18, 259–269.
Toledo Perdomo, K., Navarro Cabello, M.D., Perez Saez, M.J., Ramos Perez, M.J., Aguera Morales, M.L., Aljama Garcia, P., 2012. Reversible acute encephalopathy with mutism, induced by calcineurin inhibitors after renal transplantation. J. Nephrol. 25, 839–842.
Unadkat, J.V., Schnider, J.T., Feturi, F.G., Tsuji, W., Bliley, J.M., Venkataramanan, R., Solari, M.G., Marra, K.G., Gorantla, V.S., Spiess, A.M., 2017. Single implantable FK506 disk prevents rejection in vascularized composite allotransplantation. *Plast. Reconstr. Surg.* 139, 403e–414e.
VAN DER Merwe, Y., Steketee, M.B., 2016. Immunomodulatory approaches to CNS injury: extracellular matrix and exosomes from extracellular matrix conditioned macrophages. Neural Regen. Res. 11, 554–556.
VAN Noort, R., Black, M.M., Martin, T.R., Meanley, S., 1981. A study of the uniaxial mechanical properties of human dura mater preserved in glycerol. Biomaterials 2, 41–45.
Varghese, J., Reddy, M.S., Venugopal, K., Perumalla, R., Narasimhan, G., Arikichenin, O., Shanmugam, V., Shanmugam, N., Srinivasan, V., Jayanthi, V., Rela, M., 2014. Tacrolimus-related adverse effects in liver transplant recipients: its association with trough concentrations. Indian J. Gastroenterol. 33, 219–225.
Voda, J., Yamaji, T., Gold, B.G., 2005. Neuroimmunophilin ligands improve functional recovery and increase axonal growth after spinal cord hemisection in rats. J. Neurotrauma 22, 1150–1161.
Wakita, H., Tomimoto, H., Akiguchi, I., Kimura, J., 1998. Dose-dependent, protective effect of FK506 against white matter changes in the rat brain after chronic cerebral ischemia. Brain Res. 792, 105–113.
Wang, M.S., Gold, B.G., 1999. FK506 increases the regeneration of spinal cord axons in a predegenerated peripheral nerve autograft. J. Spinal Cord Med. 22, 287–296.
Xu, X., Su, B., Barndt, R.J., Chen, H., Xin, H., Yan, G., Chen, L., Cheng, D., Heitman, J., Zhuang, Y., Fleischer, S., Shou, W., 2002. FKBP12 is the only FK506 binding protein mediating T-cell inhibition by the immunosuppressant FK506. Transplantation 73, 1835–1838.
Yamazoe, K., Yamazoe, K., Yamaguchi, T., Omoto, M., Shimazaki, J., 2014. Efficacy and safety of systemic tacrolimus in high-risk penetrating keratoplasty after graft failure with systemic cyclosporine. Cornea 33, 1157–1163.
Yang, R.K., Lowe III, J.B., Sobol, J.B., Sen, S.K., Hunter, D.A., Mackinnon, S.E., 2003. Dose-dependent effects of FK506 on neuroregeneration in a rat model. Plast. Reconstr. Surg. 112, 1832–1840.
Zawadzka, M., Kaminska, B., 2005. A novel mechanism of FK506-mediated neuroprotection: downregulation of cytokine expression in glial cells. Glia 49, 36–51.
Zawadzka, M., Dabrowski, M., Gozdz, A., Szadujkis, B., Sliwa, M., Lipko, M., Kaminska, B., 2012. Early steps of microglial activation are directly affected by neuroprotectant FK506 in both in vitro inflammation and in rat model of stroke. J. Mol. Med. (Berl.) 90, 1459–1471.